ISSN 1814-4225 (print)
ISSN 2663-2012 (online)

UDC 629.735.45.054.42:004.8 **doi: 10.32620/reks.2023.3.05**

Dmytro VLASENKO, Olha INKABAIEVA, Maksym PERETIATKO, Danyil KOVALCHUK, Oleksandr SEREDA

National Aerospace University "Kharkiv Aviation Institute", Kharkiv, Ukraine

HELICOPTER RADIO SYSTEM FOR LOW ALTITUDES AND FLIGHT SPEED MEASURING WITH PULSED ULTRA-WIDEBAND STOCHASTIC SOUNDING SIGNALS AND ARTIFICIAL INTELLIGENCE ELEMENTS

*The **subject matter** of this study is algorithms for measuring the components of an aircraft speed vector and altitude. The **goal** of this study is to improve algorithms for processing wideband stochastic pulse signals in helicopter low-altitude and flight-speed radio systems by introducing secondary signal processing based on artificial intelligence elements. The **tasks** to be solved are as follows: to develop an optimal algorithm for determining the speed and altitude of flight for a helicopter radio complex; to supplement the signal processing algorithm with an artificial intelligence-based processor to determine the "safety" of the current trajectory; provide the pilot with relevant information about possible options for further actions based on an analysis of the current position of the helicopter and flight parameters; and to analyse the efficiency of the proposed complex when using various artificial intelligence-based algorithms. The **methods** used are as follows: methods of mathematical statistics and optimal solutions for solving problems of statistical synthesis of active radio complex structure; methods of machine learning; and methods of computer simulation. The following **results** were obtained. The algorithms for signal processing in a helicopter radio complex are obtained by the method of maximum likelihood, and the use of three radio channels to calculate the full vector of speed and altitude is argued. The structure of a secondary information processing system, using algorithms based on artificial intelligence is proposed. The effectiveness of determining the safety of the current landing trajectory using various algorithms based on artificial intelligence (LinearSVC, GaussianNB, DecisionTreeClassifier, RandomForestClassifier, KNeighborsClassifier, MLPClassifier and RidgeClassifier) was analysed. **Conclusions.** The simulation results show that in the presence of accurate (noise-free) information on the current location of the helicopter, its axial velocities, and a map of the terrain with defined areas dangerous for landing, the DecisionTreeClassifier and RandomForestClassifier algorithms can provide a high probability of correctly determining the safety of the current landing trajectory. At the same time, in the presence of instability in the measurements of helicopter movement parameters, only the RandomForestClassifier algorithm maintains high accuracy.*

Keywords: *signal processing algorithm; onboard altitude radar; optimal algorithm; machine learning; artificial intelligence.*

Introduction

Motivation. Today, aviation is one of the most technologically advanced modes of transport that continues to develop rapidly. Different types of aircraft are used in many areas, ranging from civilian cargo transportation to military applications. However, despite their widespread use, aircraft have some of the highest requirements for pilot and maintenance personnel training and onboard systems for various purposes. This is because any, even a minor, pilot error, equipment malfunction, etc. can cause an airplane crash [1, 2].

Currently, significant efforts of various organizations and manufacturers are aimed at reducing operational safety risks in aviation [3]. As can be seen from the ICAO statistics [4], since 2013, the number of accidents has decreased by about 40% and has a downward trend. This decrease can be partially attributed to the development of onboard systems that can provide pilots with more accurate information about the current state of the aircraft and flight parameters and eliminate some of their errors during control [5, 6]. Particular attention is paid to the safe landing of the aircraft, since 267 significant accidents out of 782 (34%) since 2013 occurred at this stage of the flight [4]. To reduce the accident rate at this stage, various automatic landing systems are being actively developed and tested [7, 8]. However, they mostly require specially equipped sites, which is not achievable for all types of air transport, including helicopters.

Thus, an important feature of helicopters is their ability to land on unequipped sites with limited free space. This requires both high pilot skill and the acquisition of information from a significant number of onboard systems, including radio altimeters and flight speed meters [9, 10]. Currently, these are mostly two separate onboard active radio systems that use narrowband signals, with some limitations. The separation of these systems increases their overall weight and size and power consumption, which is extremely undesirable for aviation systems. When helicopters are used in wartime (even when far from the front), narrowband signals can be easily jammed by the enemy. This does not allow pilots to safely using radio systems during flight and landing, which significantly increases the possibility of accidents. Therefore, the current task is to develop algorithms and structure of a single complex capable of measuring both helicopter altitude and speed, which will significantly reduce the weight and dimensions of the system. It is also advisable to provide for work with wideband noise sensing signals [11, 12] and the use of AI-based piloting assistance algorithms [13]. This will make the operation of the complex invisible to radio reconnaissance and reduce the probability of an accident in critical situations when the possibility of a pilot's error is greatest.

State of the Art. In [14], the problem of designing an algorithm for processing wideband stochastic pulse signals and developing a relevant structural scheme for a helicopter radio altimeter was solved. The development of the ideas and approaches set forth in [14] was obtained in [15], where signal-processing algorithms were synthesized for a helicopter radio complex of low altitudes and flight speeds, and an indirect method was proposed to measure altitude. Simulation has confirmed that such a complex [15] provides measurement of three components $\{V_x(t), V_y(t), V_z(t)\}$ velocity vector $\vec{V}(t)$ and flight altitude $h(t)$ of the helicopter. In contrast to the known methods for determining velocity components [16, 17], the approach proposed in [15] works with pulsed ultra-wideband noise signals [18, 19]. This provides a double effect. It increases the stealth of advanced helicopter equipment (by reducing the reliability of radio registration) and increases the accuracy of range measurement to the elements of the underlying surface. The disadvantage of using pulsed stochastic signals is the difficulty of determining the threshold for their detection [20], and the fact that their shape "scatters" when operating at a range of several km, after which it is not possible to perform coherent signal processing. This disadvantage is not fundamental for a radio complex with low altitudes and flight speeds, but for the unification of the system (ensuring arbitrary distances of operation), it is advisable to use signals with a large base [21, 22].

Another disadvantage of the signal-processing algorithm in [15] is the lack of sensitivity for detecting vertically oriented objects in the landing zone (tree, mast, etc.). This is because of the peculiarities of using an indirect method for measuring flight altitude. Such an indirect method does not require irradiation of the area of the underlying surface directly under the helicopter and is insensitive to some objects during a vertical landing.

Objectives. This article proposes to improve the structural scheme of the helicopter radio complex [15] by introducing artificial intelligence elements into the algorithms for signal secondary processing [23, 24]. In this case, considerable attention will be paid to two approaches. The first is to consider a priori data on the underlying surface and use digital image processing methods [25, 26], and the second is to detect indirect signs of the presence of an object in the landing zone, which is similar to the ideas presented in [27]. In both cases, the decision-making process for safe landing is based on elements of artificial intelligence [28, 29].

Initial data. Description of the problem geometry and the main parameters

The geometry of the problem of synthesizing a helicopter radio complex for low altitudes and flight speeds [15] is shown in Fig. 1.

In Fig. 1, the following notations are introduced: coordinate system $0xyz$ is associated with the underlying surface (the plane $x0y$ passes through the average height of the underlying surface irregularities); the coordinate system $0'x'y'(z-h')$ is associated with the underlying surface (the plane $x'0'y'$ passes through the phase center of the helicopter antenna system and is parallel to the plane $x0y$); A_1, A_2 are transmitting and receiving antennas; h' is a flight altitude; φ_i' are angles in the picture plane on the underlying surface between the direction of flight and the projections of the axes of the directional diagrams onto the underlying surface ($i=1,2,3$); μ_i' are angles between the direction into the nadir and the corresponding beam of the radiation pattern (measured from the axis of the radiation pattern); $\vec{V}_a'$ is a helicopter speed vector.

When synthesizing the signal processing algorithm in [15], a hypothesis was applied that assumes knowledge of the law of change in the range of the underlying surface elements for each beam of the pattern. For this purpose, Fig. 1 shows three points L_i ($i=1,2,3$), which move along the arrows and go to the point L_i' when the helicopter is moving. This movement of the points is observed because real radiation patterns always have a width differently from the delta function. With this movement, the point constantly changes its range within the irradiated area by moving along lines of equal ranges.

Radioelectronic and Computer Systems, 2023, no. 3(107)
ISSN 1814-4225 (print)
ISSN 2663-2012 (online)

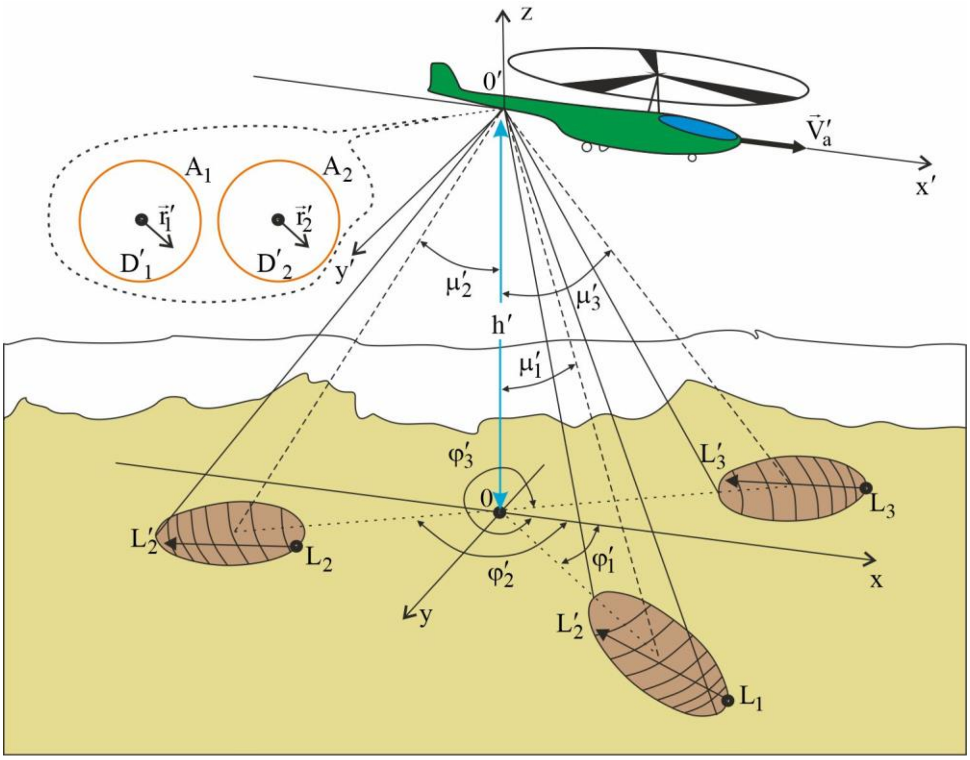

Fig. 1. Geometric relationships used for speed and altitude measurements

To determine the law of range change we need to refer to Fig. 2. In Fig. 2 the following notations have been added: R_{min}, R_{max} are minimum and maximum range within the irradiated area of the underlying surface; R_{fl} is a continuous range of the point L.

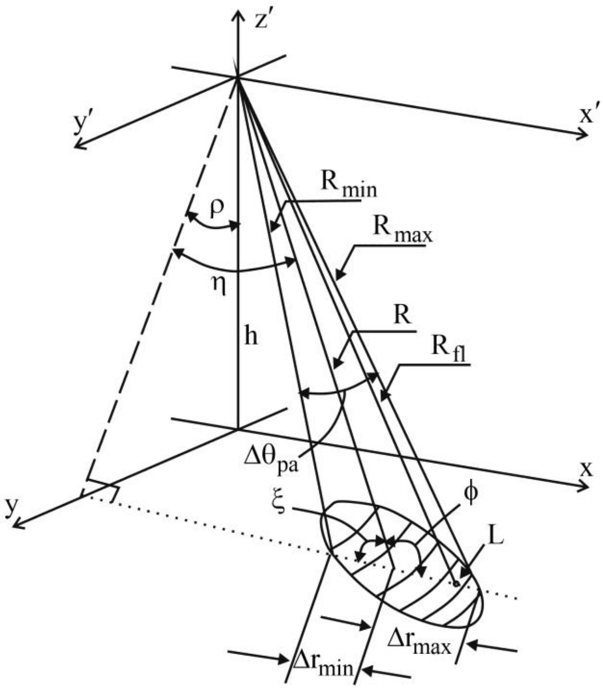

Fig. 2. Geometry for determining the law of range change during point L migration within the irradiated area of the underlying surface

Other angles on the Fig 2 have no individual values and are mathematically defined below:

$$\rho = \arctan\left(\frac{y_K}{z_K}\right), \tag{1}$$

$$\eta = \arccos\left(\frac{h}{\left|\vec{R}(\cdot)\right|\cos(\rho)}\right), \tag{2}$$

$$\xi = \frac{\pi}{2} - \eta, \tag{3}$$

$$\phi = \pi - \xi = \frac{\pi}{2} + \eta. \tag{4}$$

In (1) the following notations are added

$$\begin{aligned} y_K(t) &= h'(t)\,\mathrm{tg}(\mu')\sin(\varphi'+\alpha'(t))\cos(\chi'''(t)) + \\ &+ h'(t)\,\mathrm{tg}(\mu')\cos(\varphi'+\alpha'(t))\sin(\theta''(t))\sin(\chi'''(t)) + \\ &+ h'(t)\cos(\theta''(t))\sin(\chi'''(t)), \end{aligned} \tag{5}$$

$$\begin{aligned} z_K(t) &= h'(t)\,\mathrm{tg}(\mu')\sin(\varphi'+\alpha'(t))\sin(\chi'''(t)) - \\ &- h'(t)\,\mathrm{tg}(\mu')\cos(\varphi'+\alpha'(t))\sin(\theta''(t))\cos(\chi'''(t)) - \\ &- h'(t)\cos(\theta''(t))\cos(\chi'''(t)), \end{aligned} \tag{6}$$

where we assume that the height $h'(t)$, yaw angles $\alpha'(t)$, pitch roll $\theta''(t)$ and roll $\chi'''(t)$ of the helicopter are functions of time.

In (2) we add the range designation from the phase center of the antenna system to the center of the irradiated area (measured along the axis of the antenna pattern)

$$R(\alpha',\theta'',\chi''',h',\mu',\varphi',t)=\left|\vec{R}(\cdot)\right|=$$
$$=\frac{h'(t)\sqrt{x_K^2(t)+y_K^2(t)+z_K^2(t)}}{z_K^2(t)},\qquad(7)$$

were

$$x_K(t)=h'(t)\,tg(\mu')\cos(\varphi')\cos(\alpha'(t))\cos(\theta''(t))-$$
$$-h'(t)\,tg(\mu')\sin(\varphi')\sin(\alpha'(t))\cos(\theta''(t))-$$
$$-h'(t)\sin(\theta''(t)).\qquad(8)$$

When the analytical equations (1)-(8) have been determined, consider the equation for the change in the range law of a point L (an elementary area on the underlying surface) when the helicopter is moving:

a) for the rays directed to the front hemisphere:

$$\left|\vec{R}_{fl}(\alpha',\theta'',\chi''',h',\mu',\varphi',t)\right|=$$
$$=\left[\left|\vec{R}(\cdot)\right|^2+\left(\left|\vec{R}(\cdot)\right|\frac{\sin\left(\frac{\Delta\theta_{pa}}{2}\right)}{\sin\left(\frac{\pi}{2}-\eta-\frac{\Delta\theta_{pa}}{2}\right)}-\left|\vec{V}\right|t\right)^2-\right.$$
$$\left.-2\left|\vec{R}(\cdot)\right|\left(\left|\vec{R}(\cdot)\right|\frac{\sin\left(\frac{\Delta\theta_{pa}}{2}\right)}{\sin\left(\frac{\pi}{2}-\eta-\frac{\Delta\theta_{pa}}{2}\right)}-\left|\vec{V}\right|t\right)\cos(\phi)\right]^{0.5};\ (9)$$

b) for a ray directed into the rear hemisphere:

$$\left|\vec{R}_{fl}(\alpha',\theta'',\chi''',h',\mu',\varphi',t)\right|=$$
$$=\left[\left|\vec{R}(\cdot)\right|^2+\left(\left|\vec{R}(\cdot)\right|\frac{\sin\left(\frac{\Delta\theta_{pa}}{2}\right)}{\sin\left(\frac{\pi}{2}-\eta+\frac{\Delta\theta_{pa}}{2}\right)}-\left|\vec{V}\right|t\right)^2-\right.$$
$$\left.-2\left|\vec{R}(\cdot)\right|\left(\left|\vec{R}(\cdot)\right|\frac{\sin\left(\frac{\Delta\theta_{pa}}{2}\right)}{\sin\left(\frac{\pi}{2}-\eta+\frac{\Delta\theta_{pa}}{2}\right)}-\left|\vec{V}\right|t\right)\cos(\xi)\right]^{0.5}.\ (10)$$

Calculate the derivative of the law of range change and determine the speed. However, it should be noted that the derivative of this range will give the relative speed of the point's L and helicopters approach. Therefore, to calculate the speed of a helicopter, the following computations must be performed:

$$V_a(t)=\frac{\frac{d}{dt}\left|\vec{R}_{fl}(\alpha',\theta'',\chi''',h',\mu',\varphi',t)\right|}{\cos(\xi)}.\qquad(11)$$

To determine the components $V_x(t)$, $V_y(t)$, $V_z(t)$ velocity vector $\vec{V}_a$ the following operations must be performed to process the speeds:

$$V_x(t)=\frac{V_2(t)-V_3(t)}{2};$$
$$V_y(t)=\frac{V_1(t)-V_2(t)}{2};$$
$$V_z(t)=\frac{dh(t)}{dt},\qquad(12)$$

where $V_i(t)$ ($i=1,2,3$) are the velocities calculated from the corresponding rays, and the height is computed through the ranges as follows

$$h(t)=\frac{R_1(\cdot,t)R_3(\cdot,t)}{\sqrt{R_1^2(\cdot,t)+R_3^2(\cdot,t)-2R_1(\cdot,t)R_3(\cdot,t)\cos(2\mu')}},\qquad(13)$$

where $R_i(\cdot,t)$ are distances calculated in accordance with (7) on the i-th ray.

The emitted signal. Equation of observation. Algorithm for processing the received signals

In [15], we use the following emitted signal form:

$$s(t)=A\left(tT_s^{-1}\right)\mathrm{Re}\exp\left(j2\pi\left(f_0t+0.5\alpha t^2\right)\right),(14)$$

where $A\left(tT_s^{-1}\right)$ is signal envelope; T_s is a signal (pulse) duration; f_0 is a frequency of the emitted signal, $\alpha=(F_{max}-F_{min})T_s^{-1}$; F_{max} and F_{min} are maximum and minimum frequencies in the operating frequency spectrum.

The signal received by the antenna (one i-th ray of the radiation pattern) is presented in the following form

 ISSN 1814-4225 (print)
ISSN 2663-2012 (online)

$$s_i(t)=\operatorname{Re}\int_{D_i}\dot{F}(\vec{r})\left|\dot{G}(\vec{r})\right|^2 A\left(t-2\left|\vec{R}_{fl}(t,\vec{r})\right|c^{-1}\right)\times$$
$$\times\exp\left(j2\pi\left[\begin{array}{c} f_0\left(t-2\left|\vec{R}_{fl}(t,\vec{r})\right|c^{-1}\right)+ \\ +0.5\alpha\left(t-2\left|\vec{R}_{fl}(t,\vec{r})\right|c^{-1}\right)^2\end{array}\right]\right)d\vec{r}, \quad (15)$$
$$i=1,2,3,$$

where $\dot{F}(\vec{r})=\left|\dot{F}(\vec{r})\right|\exp\left(j\xi(\vec{r})\right)$ is a complex reflection coefficient of the underlying surface; $\xi(\vec{r})$ is a random phase taper during reflection from the underlying surface; D_i is the area of the underlying surface irradiated by the radiation pattern $\dot{G}(\vec{r})$; c is the speed of light; $\left|\vec{R}_{fl}(t,\vec{r})\right|$ is determined in accordance with (9) or (10) considering that the angles $\alpha',\theta'',\chi''',h',\mu',\varphi'$ are uniquely associated with the radius vector $\vec{r}\in(x,y)$, which characterizes the position of the irradiated elemental area on the underlying surface relative to the coordinate origin.

Signal (15) is observed against the background of internal interference of the receiver. Therefore, the observation equation can be represented in the additive form of the signal and noise

$$u_i(t)=s_i(t)+n_i(t),\ i=1,2,3, \quad (16)$$

where $n(t)$ is a white Gaussian noise (internal receiver noise) with power spectral density $0.5N_0$ and the correlation function

$$R_{nij}(t_1,t_2)=\left\langle n_i(t_1)n_j(t_2)\right\rangle=0.5N_0\delta(t_1-t_2)\delta_{ij};$$

$\delta(t_1-t_2)$ is a delta function; δ_{ij} is the Kronecker symbol [30].

The peculiarity of the problem to be solved is optimization with reference to the process evaluation, specifically the law of range change $R_{fl,i}(\vec{r})=\left|\vec{R}_{fl,i}(\vec{r})\right|$ for each range band within the irradiated area of the underlying surface (see Fig. 2). In this case, the likelihood equation takes the form

$$\frac{\delta\ln p\left(u_i(t)\,|\,R_{fl,i}(t,\vec{r})\right)}{\delta R_{fl,i}(\vec{r})}=\frac{\delta k}{\delta R_{fl,i}(\vec{r})}-$$
$$-\frac{1}{N_0}\frac{\delta}{\delta R_{fl,i}(\vec{r})}\int_0^{T_s}\left(u_i(t)-s_i\left(t,R_{fl,i}(t,\vec{r})\right)\right)^2dt=0.$$

After differentiation it can be represented as follows:

$$\int_0^{T_s}s_i\left(t,R_{fl,i}(t,\vec{r})\right)\frac{\delta}{\delta R_{fl,i}(\vec{r})}s_i\left(t,R_{fl,i}(t,\vec{r})\right)dt=$$
$$=\int_0^{T_s}u_i(t)\frac{\delta}{\delta R_{fl,i}(\vec{r})}s_i\left(t,R_{fl,i}(t,\vec{r})\right)dt. \quad (17)$$

The left side is the mathematical expectation of the right side; therefore, (17) is an equation, not an equality. The left side can be viewed as an ambiguity function of the system, provided that in signal (15) we take $\dot{F}(\vec{r})=\delta(\vec{r}-\vec{r}')$, where $\delta(\vec{r}-\vec{r}')$ is a spatial delta function.

Range estimation $\hat{R}_{fl}(t,\vec{r})$ can be obtained on the basis of (17) in the form of the following variational derivative:

$$\frac{\delta}{\delta R_{fl,i}(\vec{r})}s_i\left(t,R_{fl,i}(t,\vec{r})\right)=$$
$$=\operatorname{Re}\int_{D_i}\dot{F}(\vec{r})\left|\dot{G}(\vec{r})\right|^2\left[\frac{\delta}{\delta R_{fl,i}(\vec{r})}A\left(t-\frac{2R_{fl,i}(t,\vec{r})}{c}\right)\right]\times$$
$$\times\exp\left(j2\pi\left[f_0\left(t-\frac{2R_{fl,i}(t,\vec{r})}{c}\right)+\right.\right.$$
$$\left.\left.+\frac{\alpha\left(t-2R_{fl,i}(t,\vec{r})c^{-1}\right)^2}{2}\right]\right)d\vec{r}+\operatorname{Re}(-j)2\pi\dot{F}(\vec{r})\times$$
$$\times\left|\dot{G}(\vec{r})\right|^2A\left(t-\frac{2R_{fl,i}(t,\vec{r})}{c}\right)\times\left\{\frac{2f_0}{c}+\frac{2\alpha t}{c}-\right.$$
$$\left.-\frac{4\alpha R_{fl,i}(t,\vec{r})}{c^2}\right\}\exp\left(j2\pi\left[f_0\left(t-\frac{2R_{fl,i}(t,\vec{r})}{c}\right)+\right.\right.$$
$$\left.\left.+\frac{\alpha\left(t-2R_{fl,i}(t,\vec{r})c^{-1}\right)^2}{2}\right]\right). \quad (18)$$

If we have information about the range $\hat{R}_{fl}(t,\vec{r})$, helicopter speed $V_a(t)$ can be further estimated using formula (11). However, the information obtained from only one beam of the radiation pattern is not sufficient to calculate the full helicopter velocity vector and its height using formulas (12) and (13). To achieve this, two additional measurement channels must be added to the system with radiation patterns pointing in different directions relative to each other, as shown in Figure 1.

Then, on the basis of the range estimates of the three channels, it is possible to calculate the flight speeds $V_x(t)$, $V_y(t)$, $V_z(t)$ and height $h(t)$. Subsequently, the pilot or the onboard automatic control system to adjust the flight and avoid emergencies can use the information obtained.

.

Simulation of the algorithms for warning about dangerous helicopter landing trajectories

In the previous section, algorithms for measuring helicopter movement parameters were obtained, which the pilot for safe maneuvers subsequently analyzed. All measurements have errors resulting from internal receiver noise, various destabilizing factors, and radio interference. These errors distort information about the helicopter's position in space. In addition, the change in spatial position can be affected by errors in the operation of spatial stabilization systems and bad weather conditions, particularly squally gusts of wind. The secondary processing of the measurement results in a certain time can reduced the influence of these factors. The synthesis of secondary processing algorithms can be performed by statistical optimization methods of filtering algorithms or modern methods of artificial intelligence. Next, this article considers the possibilities of machine learning methods for analyzing trajectories and providing information to the pilot about dangerous helicopter trajectories despite interference.

Aviation accident statistics show that most helicopter accidents occur during takeoff and landing. Thus, for further analysis, we considered the current situation of helicopters landing on different trajectories, indicating critical ones in terms of overloads or descent angles. In addition, onboard optical vision systems at night and in bad weather do not allow the pilot to visualize the surface to make a decision on choosing a safe landing site. In this case, it is advisable to have a map of the terrain with marked safe zones, a system for calculating the landing point based on current trajectories, and algorithms for warning of dangerous trajectories, which are integrated into the pilot's decision support system.

The idea of improving the helicopter's control system can be implemented as follows. Data from the radio engineering complex for measuring flight parameters (speed, altitude, and drift angles) are transmitted to an artificial intelligence processor. This processor also receives a periodically updated terrain map. Using digital image processing methods, the map identifies areas that pose a danger to the helicopter landing (areas with a slope of more than 3 degrees, infrastructure, forest plantations and individual trees, and water bodies). In addition, the processor considers the restrictions imposed on the trajectories of this type of helicopter due to its tactical and technical characteristics. Next, artificial intelligence algorithms in the processor, controlling the current flight parameters, calculate the current trajectory and landing site. The calculation results are compared with a digital map with preclassified areas that are conditionally "safe" for landing and "unsafe" for landing. If the trajectory is classified as dangerous, the pilot is given a warning about the dangerous trajectory in advance and is offered actions to correct it for a safe landing. A block diagram of the described system for secondary processing of measurement results is shown in Fig. 3.

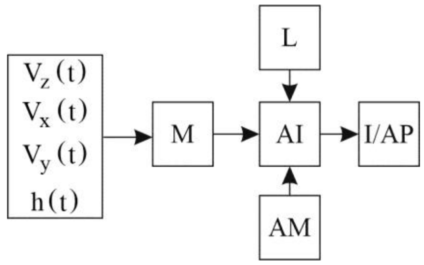

Fig. 3. Block diagram of the system secondary processing of the measurement results

In Fig. 3 AI is an artificial intelligence processor; AM is an area map; I/AP is an indicator or autopilot system; L is limitations of the helicopter's flight characteristics; block M determines the system operation mode.

To validate the proposed approach, we performed simulations of various algorithms and modeled two-dimensional trajectories and studied the performance of a few machine learning methods for the classification task. An example of the trajectories analyzed is shown in Fig. 4.

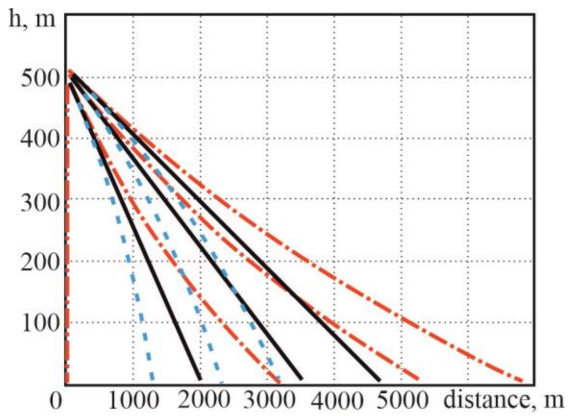

Fig. 4. Examples of helicopter landing trajectories from the database of possible trajectories

Two components are needed to train ML (machine learning) algorithms: "features" and "labels". "Labels"

ISSN 1814-4225 (print)
ISSN 2663-2012 (online)

are the results we want to obtain from the model. In this case, whether the current trajectory is safe for landing or not, they are obtained by comparing a set of trajectories and a digital map. "Signs" are the array of information that is usually collected during the operation of a particular system (or generated on the basis of known operating conditions) and from which one can distinguish the actual signs that can directly or indirectly affect the above-mentioned "labels".

In this study, the "marks" and "signs" were independently formed according to typical models of helicopter landing trajectories, as shown in Fig. 4. In the future, these data will be obtained experimentally from the onboard systems of Motor Sich helicopters. The "labels" and "signs" were formed according to the following algorithm.

1. A database of landing trajectories based on the current position and Two components are needed to train ML (machine learning) algorithms: "features" and "labels". "Labels" are the results we want to obtain from the model. In this case, whether the current trajectory is safe for landing or not, they are obtained by comparing a set of trajectories and a digital map. "Signs" are the array of information that is usually collected during the operation of a particular system (or generated on the basis of known operating conditions) and from which one can distinguish the actual signs that can directly or indirectly affect the above-mentioned "labels".

In this study, the "marks" and "signs" were independently formed according to typical models of helicopter landing trajectories, as shown in Fig. 4. In the future, these data will be obtained experimentally from the onboard systems of Motor Sich helicopters. The "labels" and "signs" were formed according to the following algorithm $V_x(t)$ i $V_z(t)$. The trajectories are shown graphically in Fig 4.

2. A conditional digital map with highlighted areas of "dangerous landing" was constructed (Figure 5). Because we are considering a simplified two-dimensional case, only one line from this map is used in the following. In practice, such a map can be quickly created.

Fig. 5. Digital map of the area after processing

3. Trajectories that are recognized as unsafe based on helicopter operating conditions (too high or low speed for landing, critical angles) are marked as "unsafe" in the trajectory database.

4. By comparing the endpoints of the trajectories with the points on the map, the trajectories that lead to landing in dangerous areas were identified (accordingly, their status in the trajectory database is indicated as "dangerous")

5. The data for training is generated using the Octave environment. The result is a two-dimensional matrix in which the bulk of the columns represent the parameters of the trajectory points, and the last column is the "labels" in binary form (0 is "safe" trajectory, 1 is "dangerous" trajectory). Subsequently, the matrix is written to a file in the format CSV.

6. Machine learning models were trained in the Spyder programming environment of the specialized Anaconda Navigator package with the numpy, pandas, and scikit-learn libraries.

In the first step, the CSV file is divided into arrays of features. The "features" is used for training and labeling, where "labels" are the results that we want to train the model to predict. Next, these arrays are divided into training and testing samples in the proportion of 75% to 25%.

7. The next step is to download the ML models from the scikit-learn library. The following models have been added: LinearSVC, GaussianNB, DecisionTreeClassifier, RandomForestClassifier, KNeighborsClassifier, MLPClassifier, and RidgeClassifier.

LinearSVC is a linear classification model. It is used for binary and multiclass classification tasks. It works by finding the hyperplane that best separates the classes in the training data. Gaussian Naive Bayes is a probabilistic classification algorithm. It assumes that the features are normally distributed and independent. A Decision Tree is a tree-like model used for both classification and regression tasks. It partitions the data into subsets based on the values of features to minimize impurities. RandomForest is an ensemble learning method that combines multiple decision trees to improve accuracy and reduce overfitting. It works by aggregating the predictions of the individual decision trees. K-Nearest Neighbors is a lazy learning algorithm used for classification tasks. It assigns a class label to an instance based on the majority class among its k-nearest neighbors in the training data, where k is a user-defined parameter. MLP is an artificial neural network commonly used for classification tasks. It consists of multiple layers of interconnected nodes (neurons) and can learn complex patterns in data. RidgeClassifier is a linear classifier that uses L2 regularization (ridge regression) to prevent overfitting. Implementations of these algorithms, which are part of the scikit-learn package [31], were used in this study.

These models were trained on a training set of "features" and "labels". The training curve for the RandomForestClassifier algorithm is shown in Fig. 6.

After training, the trained models were tested by providing them with only "features" and obtaining predicted "labels". To assess the quality of the work, the percentage of correct predictions for the trained models was calculated (Table 1).

Based on the obtained estimates, we can conclude that the accuracy of the presented algorithms in the task context is quite high. Thus, given parameters such as the current position, terrain map, and axial velocities, machine learning algorithms can be used to determine whether the current descent trajectory is safe for landing.

The analysis of the scores shows that some machine learning models are not suitable for this task. The best results were obtained using the model RandomForest (accuracy: 91.5 %) i DecisionTree (accuracy: 91.5 %).

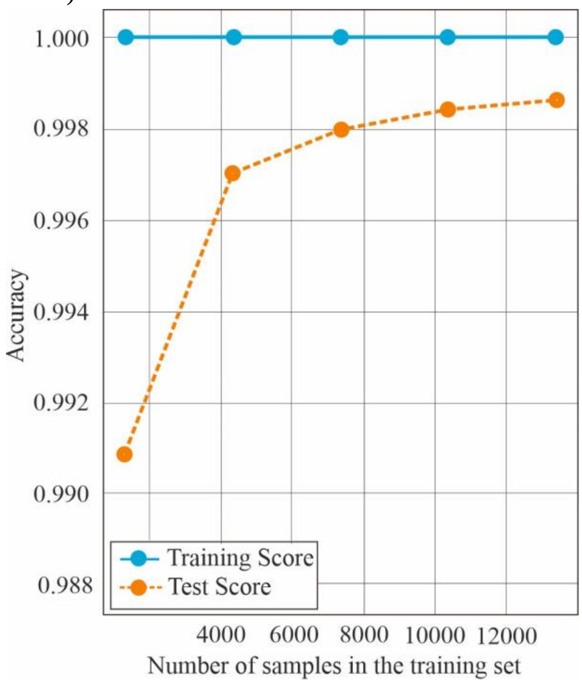

Fig. 6. Training curve for the algorithm RandomForestClassifier

Table 1

Percentage of correct predictions for different machine learning models

Model name	Correct prediction in %
LinearSVC	52.3
GaussianNB	43.1
DecisionTreeClassifier	91.5
RandomForestClassifier	91.5
KNeighborsClassifier	76.0
MLPClassifier	51.3
RidgeClassifier	51.3

Next, consider these two algorithms when working in noise.

Further research is performed under the assumption that the training was performed on ideal trajectories, and it is advisable to test the developed algorithms in the presence of noise (wind gusts) that changes the shape of the trajectory. Such factors are quite difficult to account for when tuning the parameters of machine learning models. We use additive Wiener noise, which is generally a Markov process of the first kind. Wiener noise was generated in Octave as an integral of white Gaussian noise. Examples of trajectories with different levels of Gaussian noise variance are shown in Fig. 7.

The test results of the RandomForest and DecisionTree algorithms for the variance level of Gaussian noise from 1 to 100 are shown in Fig. 8

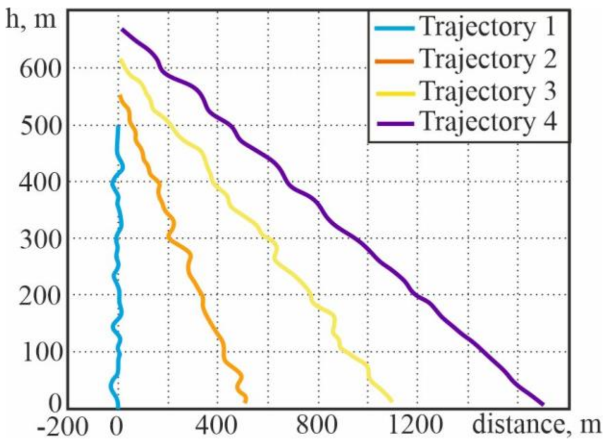

a

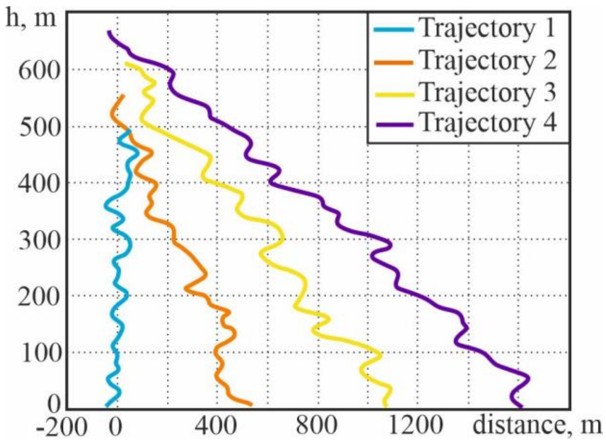

b

Fig. 7. Helicopter landing trajectories accounting for the influence of additive noise:
a – noise variance is 3 m;
b – noise variance is 10 m

Discussion

From the analysis of the data obtained, it follows that when changing the measurement errors of helicop-

 ISSN 1814-4225 (print)
ISSN 2663-2012 (online)

ter movement parameters and increasing the accuracy of spatial stabilization means, it is possible to use either of the two methods considered, since the accuracy of detecting dangerous trajectories at low noise levels is 91.5%. In the case when there is a probability of unstable helicopter flight, it is more appropriate to use the RandomForestClassifier algorithm for the task assigned, which maintains an accuracy of at least 90% even when exposed to noise with a dispersion of 35.

It should also be noted that to reduce the impact of noise on the results of the algorithms, it is advisable to perform secondary data processing. To do this, it is possible to either calculate new filtering algorithms that are optimal for the system under consideration or adapt existing filters, such as those used for image processing [32].

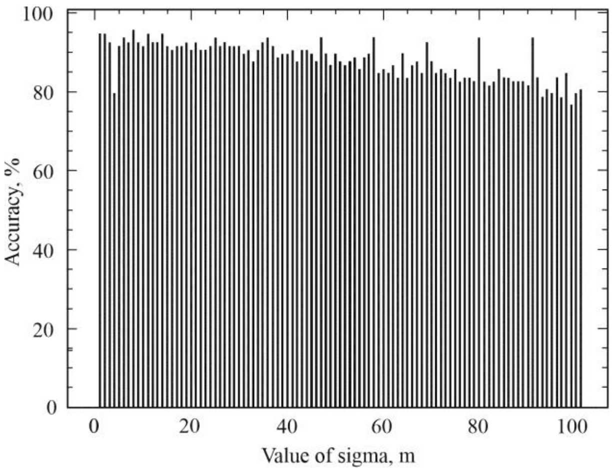

a

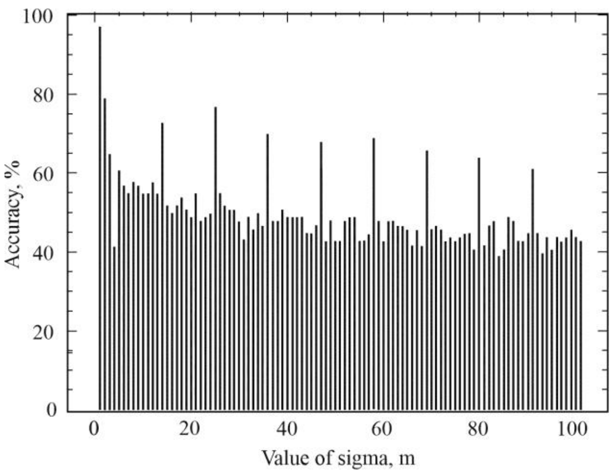

b

Fig. 8. Testing algorithms for detecting dangerous landing trajectories under the influence of noise:
a – RandomForestClassifier algorithm,
b – DecisionTreeClassifier algorithm

Conclusions

This paper considers analytical expressions for determining the components of $V_x(t)$, $V_y(t)$, $V_y(t)$ velocity vector $\vec{V}_a$ and flight altitude $h(t)$ of the aircraft. The peculiarity of the calculations is the need to use three measuring channels in the onboard radio complex, i.e., three patterns of reception and transmission formed in different directions relative to the helicopter's movement direction. By calculating the relative speed of movement, as well as the range to the underlying surface for each beam, it is possible to obtain current information on the speed of the aircraft $V_x(t)$ and $V_y(t)$, as well as the height of the flight. Subsequently, it becomes possible to determine the flight altitude as a derivative of the flight altitude.

Particular attention is paid to the secondary processing of information in the proposed radio complex. Thus, the possibility of using artificial intelligence algorithms to process information on the safety of the current helicopter flight path at the landing stage is considered. Simulation modeling was performed, during which the models LinearSVC, GaussianNB, DecisionTreeClassifier, RandomForestClassifier, KNeighborsClassifier, MLPClassifier, and RidgeClassifier were trained on examples of helicopter landing trajectories to determine the safety of the current landing trajectory, based on information about the current speed and altitude of the flight, as well as a map of the area with defined zones safe for landing. The modeling results are particularly significant for the DecisionTreeClassifier and RandomForestClassifier models, which, in the absence of noise in the measurements, provided a probability of correct prediction of 91.5%. However, in the presence of noise in the measurements, DecisionTreeClassifier loses its effectiveness. At the same time, RandomForestClassifier maintains an accuracy of at least 90% even when exposed to noise with a sufficiently high variance. The results obtained indicate the possible effectiveness of involving machine learning algorithms in solving the problem of secondary information processing in onboard radio altimeters and the feasibility of further research in this area.

Further research on this topic will be directed in several directions. Currently, software is being developed to generate different types of bedding surfaces with a given level of elevation and roughness. This will enable the simulation to replace the terrain map image, which is not always available, with a terrain map that can currently be generated in real time by the onboard radars of some aircraft. It is also planned to collaborate with Motor Sich to collect and systematize information on the landing trajectories of real helicopters. This will allow training and testing of the performance of artificial intelligence algorithms in real-world conditions.

Contribution of authors: conceptualization – **Olha Inkarbaieva**, **Dmytro Vlasenko;** methodology – **Danyil Kovalchuk**; simulation – **Dmytro Vlasenko**; validation – **Maksym Peretiatko**; formal analysis – **Oleksandr Sereda**; investigation – **Maksym Peretiatko**; resources – **Oleksandr Sereda**; data curation – **Danyil Kovalchuk**; writing original draft – **Olha Inkarbaieva**, **Dmytro Vlasenko**; writing-review and editing – **Danyil Kovalchuk**, **Oleksandr Sereda**; supervision – **Maksym Peretiatko**; project administration – **Dmytro Vlasenko**; funding acquisition – **Dmytro Vlasenko**.

All authors have read and agreed to the published version of the manuscript.

Acknowledgement. This work was funded by the Ministry of Education and Science of Ukraine. The state registration number of the project *« Domestic radar complex of low altitudes and flight speeds for helicopters JSC "Motor Sich"»* is 0122U200469. The state registration number of the project *«Design, development of a layout and experimental study of a passive radar with a noise-immune target illumination signal for detecting UAVs»* is 0123U102000.

References

1. Wang, W., Wang, J., & Lei, B. General Aviation Accident Masking Causation Based on the HFACS Model Analysis. *2023 7th International Conference on Transportation Information and Safety (ICTIS)*, 2023, pp. 2271-2276. DOI: 10.1109/ICTIS60134.2023.10243710.

2. Konieczka, R. Defines causes and the circumstance of air accidents in preparatory conducts connected with their appearing. *Transportation Overview*, 2018, no. 1, pp. 10-16. DOI: 10.35117/A_ENG_18_01_02

3. ICAO, "Global Aviation Safety Plan", available at: https://www.icao.int/safety/GASP/Pages/ Goals-and-Targets.aspx (accessed 15 Augus 2023)

4. ICAO, "Accident Statistics", available at: https://www.icao.int/safety/iStars/Pages/Accident-Statistics.aspx (accessed 15 Augus 2023)

5. Predescu, A.-V., & Stelkens-Kobsch, T. H. Aviation Security Lab: A testbed for security testing of current and future aviation technologies. *2022 IEEE/AIAA 41st Digital Avionics Systems Conference (DASC)*, 2022, pp. 1-5. DOI: 10.1109/DASC55683. 2022.9925750.

6. Yuan, Y., Yu, J., & Zhang, Y. Research on Technology Trend for Civil Aviation Safety based on Patent Big Data Analysis. *2020 IEEE 2nd International Conference on Civil Aviation Safety and Information Technology (ICCASIT)*, 2020, pp. 987-991. DOI: 10.1109/ICCASIT50869.2020.9368640.

7. Yuan, Y., Duan, H., & Zeng, Z. Automatic Carrier Landing Control With External Disturbance and Input Constraint. *IEEE Transactions on Aerospace and Electronic Systems*, 2023, vol. 59, iss. 17, pp. 1426-1438. DOI: 10.1109/TAES.2022. 3202142.

8. Vlk, J., Chudy, P., & Prustomersky, M. Light Sport Aircraft Auto-Land System. *2019 IEEE/AIAA 38th Digital Avionics Systems Conference (DASC)*, 2019, pp. 1-10. DOI: 10.1109/DASC43569.2019. 9081730.

9. Bursucianu, V., Amrhar, A., Gagné, J. -M., & Landry, R. J. RFSoC-based design and implementation of a Direct RF FMCW radar altimeter. *2023 IEEE Radar Conference (RadarConf23)*, 2023, pp. 1-6. DOI: 10.1109/RadarConf2351548.2023.10149605.

10. Hügler, P., Geiger, M., & Waldschmidt, C. 77 GHz radar-based altimeter for unmanned aerial vehicles. *2018 IEEE Radio and Wireless Symposium (RWS)*, 2018, pp. 129-132. DOI: 10.1109/RWS. 2018.8304965.

11. Pavlikov, V., Volosyuk, V., Nechyporuk, M., Sobkolov, A., Odokienko, O., & Tserne, E. Algorithm of Formation Radio Images from Aerospace Carriers. *2020 IEEE Ukrainian Microwave Week (UkrMW)*, 2022, pp. 54-58. DOI: 10.1109/UkrMW49653. 2020.9252702.

12. Ruzhentsev, N., Zhyla, S., Pavlikov, V., Volosyuk, V., Tserne, E., Popov, A., Shmatko, O., Ostroumov, I., Kuzmenko, N., Dergachov, K., Sushchenko, O., Averyanova, Y., Zaliskyi, M., Solomentsev, O., Havrylenko, O., Kuznetsov, B., & Nikitina, T. Practical imaging algorithms in ultra-wideband radar systems using active aperture synthesis and stochastic probing signals. *Radioelectronic and computer systems*, 2023, vol. 105, iss. 1, pp. 55-73. DOI: 10.32620/reks.2023.1.05.

13. Jiang, Y., Tran, T. H., & Williams, L., Machine learning and mixed reality for smart aviation: Applications and challenges. *Journal of Air Transport Management*, 2023, vol. 111, pp. 102437. DOI: 10.1016/j.jairtraman.2023.102437.

14. Volosyuk, V., Pavlikov, V., Zhyla, S., Tserne, E., Odokiienko, O., Humennyi, A., Popov, A., & Uruskiy, O. Signal Processing Algorithm for Monopulse Noise Noncoherent Wideband Helicopter Altitude Radar. *Computation*, 2022, vol. 10 iss. 9, pp. 150-166. DOI: 10.3390/computation10090150.

15. Pavlikov, V., Tserne, E., Odokiienko, O., Sydorenko, N., Peretiatko, M., Kosolapova, O., Prokofiiev, I., & Humennyi, A. Algorithm for Determining Three Components of the Velocity Vector of Highly Maneuverable Aircraft. *Computation*, 2023, vol. 11, iss. 2, pp. 35-47. DOI: 10.3390/ computation11020035.

16. Haag, M. U., Huschbeck, S., & Huff, J. sUAS Swarm Navigation using Inertial, Range Radios and Partial GNSS. *2019 IEEE/AIAA 38th Digital Avionics*

Systems Conference (DASC), 2019, pp. 1-10. DOI: 10.1109/DASC43569.2019.9081793.

17. Di Fiore, V., Conte, C., Bottino, V., Accardo, D., Rufino, D. G., de Alteriis, G., Passaniti, F., Patti, D., & Sanfilippo, D. Innovative Airspeed Sensing Based on a Micromachined Sensor. *2023 IEEE 10th International Workshop on Metrology for AeroSpace (MetroAeroSpace)*, 2023, pp. 25-30. DOI: 10.1109/MetroAeroSpace57412.2023.10189995.

18. Sytnik, O., & Vyzmitinov, I. Adaptive approach to filtering of stochastic processes in rescuer radar. *Telecommunications and Radio Engineering*, 2021, vol. 90, iss. 3, pp. 15-22. DOI: 10.1615/TelecomRadEng.2021037975.

19. Sytnik, O. V. Jitter Problem in Pseudo Random Signal Processing. *Telecommunications and Radio Engineering*, 2020, vol. 79, iss. 5, pp. 425-432. DOI: 10.1615/TelecomRadEng.v79.i5.50.

20. Ruzhentsev, N., Zhyla, S., Pavlikov, V., Volosyuk, V., Tserne, E., Popov, A., Shmatko, O., Ostroumov, I., Kuzmenko, N., Dergachov, K., Sushchenko, O., Averyanova, Y., Zaliskyi, M., Solomentsev, O., Havrylenko, O., Kuznetsov, B., & Nikitina, T. Method of Optimal Threshold Calculation in Case of Radio Equipment Maintenance. *Data Science and Security. Lecture Notes in Networks and Systems*, 2022, vol. 462, iss 1, pp. 110-134. DOI: 10.1007/978-981-19-2211-4_6.

21. Shahin, K., Artin, K., & Mobin, J. Novel continuous phase DDS model for linear Chirp Signal Simulation in Pulse Compression Radar. *2021 29th Iranian Conference on Electrical Engineering (ICEE)*, 2021, pp. 798-804. DOI: 10.1109/ICEE52715.2021.9544243.

22. Alabd, M. B., de Oliveira, L. G., Nuss, B., Wiesbeck, W., & Zwick T. Time-Frequency Shift Modulation for Chirp Sequence based Radar Communications. *2020 IEEE MTT-S International Conference on Microwaves for Intelligent Mobility (ICMIM)*, 2020, pp. 1-4. DOI: 10.1109/ICMIM48759.2020.9298987.

23. . Zhang, T., Zeng, T., & Zhang, X. Synthetic Aperture Radar (SAR) Meets Deep Learning. *Remote Sensing*, 2023, vol. 15, iss. 2, article no. 303. DOI: 10.3390/rs15020303

24. Ruzhentsev, N., Zhyla, S., Pavlikov, V., Volosyuk, V., Tserne, E., Popov, A., Shmatko, O., Ostroumov, I., Kuzmenko, N., Dergachov, K., Sushchenko, O., Averyanova, Y., Zaliskyi, M., Solomentsev, O., Havrylenko, O., Kuznetsov, B., & Nikitina, T. Decision Support System Based on the ELECTRE Method. *Data Science and Security. Lecture Notes in Networks and Systems*, 2022, vol. 262, iss. 1, pp. 196-213. DOI: 10.1007/978-981-19-2211-4_26.

25. Uss, M., Vozel, B., Lukin, V., Baryshev, I., & Chehdi, K. Image noise-informative map for noise standard deviation estimation. *2011 IEEE International Conference on Acoustics, Speech and Signal Processing (ICASSP)*, 2022, pp. 961-964. DOI: 10.1109/ICASSP.2011.5946565.

26. Ponomarenko, N. N., Lukin, V. V., Egiazarian, K. O., & Astola, J. T. A method for blind estimation of spatially correlated noise characteristics. *IS&T/SPIE Electronic Imaging*, 2010, pp. 753208. DOI: 10.1117/12.847986.

27. Molchanov, P., Astola, J., Egiazarian, K., & Totsky, A. Classification of ground moving radar targets by using joint time-frequency analysis. *2012 IEEE Radar Conference*, 2012, pp. 366-371. DOI: 10.1109/RADAR.2012.6212166.

28. Wang, Z., Li, H., Wu, H., Shen, F., & Lu, R. Design of Agent Training Environment for Aircraft Landing Guidance Based on Deep Reinforcement Learning. *2018 11th International Symposium on Computational Intelligence and Design (ISCID)*, 2018, pp. 76-79. DOI: 10.1109/ISCID.2018.10118.

29. Midtfjord, A. D., Bin, R., & Huseby, A. A Decision Support System for Safer Airplane Landings: Predicting Runway Conditions Using XGBoost and Explainable AI. *Cold Regions Science and Technology*, 2022, vol. 199, pp. 1-19. DOI: 10.1016/j.coldregions.2022.103556.

30. Frankel, T. *The Geometry of Physics: An Introduction*. Cambridge, Cambridge University Press Publ., 2012. 748 p.

31. Pedregosa, F., Varoquaux, G., Gramfort, A., Michel, V., Thirion, B., Grisel, O., Blondel, M., Müller, A., Nothman, J., Louppe, G., Prettenhofer, P., Weiss, R., Dubourg, V., Vanderplas, J., Passos, A., Cournapeau, D., Brucher, M., Perrot, M., & Duchesnay, É. Scikit-learn: Machine Learning in Python. *Journal of Machine Learning Research*, 2012, vol. 12, iss. 85, pp. 2825−2830. DOI: 10.48550/arXiv.1201.0490

32. Ponomarenko, N., Lukin, V., Zriakhov, M., Egiazarian, K., & Astola, J. *Lossy compression of images with additive noise*. Berlin, Springer Publ., 2005. 381 p.

Received 15.08.2023, Accepted 20.09.2023

ВЕРТОЛІТНИЙ РАДІОКОМПЛЕКС МАЛИХ ВИСОТ І ШВИДКОСТЕЙ ПОЛЬОТУ З ОБРОБЛЕННЯМ ІМПУЛЬСНИХ НАДШИРОКОСМУГОВИХ СТОХАСТИЧНИХ СИГНАЛІВ ТА ЕЛЕМЕНТАМИ ШТУЧНОГО ІНТЕЛЕКТУ

Дмитро Власенко, Ольга Інкарбаєва, Максим Перетятько, Даниїл Ковальчук, Олександр Середа

Предметом дослідження є алгоритми вимірювання складових вектору швидкості та висоти польоту літальних апаратів. **Метою** роботи є удосконалення алгоритмів обробки широкосмугових стохастичних імпульсних сигналів у вертолітних радіокомплексах малих висот та швидкостей польоту шляхом введення вторинної обробки сигналів на основі елементів штучного інтелекту. **Завдання:** розробити оптимальний алгоритм визначення швидкості та висоти польоту для вертолітного радіокомплексу; доповнити отриманий алгоритм оброблення сигналів процесором на основі штучного інтелекту задля визначення «безпечності» поточної траєкторії, завчасного надання відповідної інформацію пілоту щодо можливих варіантів подальших дій на основі аналізу поточного положення вертольоту та параметрів польоту; проаналізувати ефективність роботи пропонованого комплексу при залученні різних алгоритмів на основі штучного інтелекту. Використовуваними **методами** є: методи математичної статистики та оптимальних рішень при вирішенні задач статистичного синтезу структур активних радіотехнічних комплексів; методи машинного навчання; методи комп'ютерного імітаційного моделювання. Отримані такі **результати.** Методом максимальної правдоподібності отримано алгоритми обробки сигналів у вертолітному радіокомплексі та аргументовано використання трьох радіоканалів для розрахунку повного вектору швидкості та висоти польоту. Запропонована структура системи вторинної обробки інформації з залученням алгоритмів на основі штучного інтелекту. Проаналізовано ефективність визначення безпечності поточної траєкторії посадки при залученні різних алгоритмів на основі штучного інтелекту (LinearSVC, GaussianNB, DecisionTreeClassifier, RandomForestClassifier, KNeighborsClassifier, MLPClassifier і RidgeClassifier). **Висновки.** У результаті імітаційного моделювання показано, що за наявності точної (без впливу шумів) інформації щодо поточного місцеположення вертольоту, його швидкостей по осям та карти місцевості з визначеними зонами, небезпечними для посадки, алгоритми DecisionTreeClassifier та RandomForestClassifier можуть забезпечувати високу ймовірність правильного визначення безпечності поточної траєкторії зниження для посадки. Водночас зазначено, що при наявності нестабільності у вимірюваннях параметрів руху вертольоту, лише алгоритм RandomForestClassifier зберігає високу точність роботи.

Ключові слова: алгоритм обробки сигналів; бортовий радіовисотомір; оптимальний алгоритм; машинне навчання; штучний інтелект.

Власенко Дмитро Сергійович – асист. каф. аерокосмічних радіоелектронних систем, Національний аерокосмічний університет ім. М. Є. Жуковського "Харківський авіаційний інститут", Харків, Україна.

Інкарбаєва Ольга Сергіївна – асист. каф. аерокосмічних радіоелектронних систем, Національний аерокосмічний університет ім. М. Є. Жуковського "Харківський авіаційний інститут", Харків, Україна.

Перетятько Максим Сергійович – асп. каф. аерокосмічних радіоелектронних систем, Національний аерокосмічний університет ім. М.Є. Жуковського "Харківський авіаційний інститут", Харків, Україна.

Ковальчук Даниїл Іванович – інж. каф. аерокосмічних радіоелектронних систем, Національний аерокосмічний університет ім. М. Є. Жуковського "Харківський авіаційний інститут", Харків, Україна.

Середа Олександр Владиславович – технік каф. аерокосмічних радіоелектронних систем, Національний аерокосмічний університет ім. М.Є. Жуковського "Харківський авіаційний інститут", Харків, Україна.

Dmytro Vlasenko – Assistant at the Department of Aerospace Radio-Electronic Systems, National Aerospace University "Kharkiv Aviation Institute", Kharkiv, Ukraine,
e-mail: d.vlasenko@khai.edu, ORCID: 0000-0002-6118-2173.

Olha Inkarbaieva – Assistant at the Department of Aerospace Radio-Electronic Systems, National Aerospace University "Kharkiv Aviation Institute", Kharkiv, Ukraine,
e-mail: o.inkarbayeva@khai.edu, ORCID: 0000-0002-2547-8241.

Maksym Peretiatko – PhD Student at the Department of Aerospace Radio-Electronic Systems, National Aerospace University "Kharkiv Aviation Institute", Kharkiv, Ukraine,
e-mail: m.peretiatko@khai.edu, ORCID: 0000-0002-3536-5355.

Danyil Kovalchuk – Engineer at the Department of Aerospace Radio-Electronic Systems, National Aerospace University "Kharkiv Aviation Institute", Kharkiv, Ukraine,
e-mail: d.i.kovaljchuk@khai.edu, ORCID: 0009-0007-6847-6610.

Oleksandr Sereda – Technician at the Department of Aerospace Radio-Electronic Systems, National Aerospace University "Kharkiv Aviation Institute", Kharkiv, Ukraine,
e-mail: o.v.sereda@student.khai.edu, ORCID: 0009-0002-7021-5077.